



OPEN Therapeutic Potential of GYY4137 in Reducing Oxidative Stress and Mortality in Experimental Decompression Sickness

Lucile Daubresse¹, Marion Marlinge^{2,3}, H el ene Lavner³, Julia-Sophie Dodivers², Alexandrine Bertaud², Simon Lledo^{2,6}, Samantha Conte², Julien Fromonot^{2,3}, Marguerite Gastaldi³, Jean Jacques Risso^{1,4}, Jean Claude Rostain², Jean Eric Blatteau^{1,5}, Nicolas Vallee¹, R egis Guieu^{2,3}✉ & Regis Guieu¹

The pathophysiology of decompression sickness (DCS) is not fully understood. Apart from bubble formation, endothelial dysfunction and reactive oxygen species (ROS) production, participate in DCS. We aimed to evaluate the redox profile (redox potential, adenosine deaminase activity (ADA), and xanthine oxidase activity (XO) and the effects of GYY4137, an H₂S donor with antiradical properties, on the mortality of mice exposed to experimental DCS. Sixty Mice were injected intraperitoneally with either GYY4137 or saline, then subjected to high pressure in a hyperbaric chamber, followed by a quick decompression. GYY4137 increased survival with a median lethal dose (LD₅₀) of 120 m compared with those injected with saline (<100 m; *p* = 0.038) but did not affect significantly ADA or XO activities. The redox potential (RP: mV) was lower in the GYY4137 group (median-range, 116[78–189]) than that in the saline group: 150[88–226], *p* = 0.04. Experimental DCS itself was associated with an increase in RP. We concluded that GYY4137 protects mice while reducing RP and ROS production. Our results seem to indicate that the reduction of the redox potential induced by the administration of H₂S donor could reduce mortality during DCS.

*Participating equally to the work.

Corresponding author: Regis Guieu, C2VN; guieu.regis@orange.fr.

Introduction

Decompression sickness (DCS) results from the formation of gas bubbles in the blood or tissues following a rapid reduction in environmental pressure^{1,2}. Its pathophysiology involves extrapulmonary bubble formation due to tissue supersaturation with dissolved gases, followed by bubble growth. Gas embolisms occur when molecular gas from pulmonary or intravascular sources enters the arterial circulation, occluding distal vessels and potentially causing severe neurological consequences if bubbles obstruct spinal or cerebral arteries¹.

Arterial or venous embolisms may result from rapid ascent during diving or, less commonly, from breath-hold diving². When decompression procedures are properly followed, the incidence ranges from 0.01% to 0.095% of dives, with a mean of 0.03% among recreational divers². DCS primarily affects the nervous system, leading to pain, paresthesia, dizziness, vertigo, muscular weakness, or altered consciousness. Clinical manifestations are often nonspecific, and DCS is frequently misdiagnosed¹. The standard treatment consists of administering 100% oxygen for several hours, with or without recompression therapy^{2,3}.

Oxygen therapy, recompression, and several experimental adjuvant treatments have been assessed, including antiplatelet agents^{4–7}, statins^{8,9}, serotonin uptake inhibitors^{10,11}, inert gases¹², perfluorocarbons¹³, beta-blockers¹⁴, and steroidal¹⁵ or non-steroidal anti-inflammatory drugs¹⁶. Endothelial dysfunction¹⁷ and oxidative stress contribute to DCS^{18,19}. In humans, DCS induces upregulation of transcripts involved in inflammation and

¹Institute of Research in Biology of the Armed Forces Health Service (IRBA), Toulon, France. ²Nutrition and Cardiovascular Research Center (C2VN), Aix-Marseille University, Marseille, France. ³Laboratory of Biochemistry, Timone Hospital, Marseille, France. ⁴Monaco Scientific Centre, Montecarlo, Monaco. ⁵Hyperbaric Medicine Department, Saint Anne Hospital, Toulon, France. ⁶Centre for Nutrition and cardiovascular Research, Aix Marseille University, INSERM, INRAE, Marseille, France. ✉email: guieu.regis@orange.fr

free radical scavenging²⁰. Oxidative stress, mediated by reactive oxygen species (ROS), likely plays a major role in morbidity and mortality. Excess ROS production by the mitochondrial respiratory chain contributes to cell death and tissue damage²¹, and bubble exposure damages mitochondrial membranes, promoting cytolysis and cell death²².

Hydrogen sulfide (H₂S) is an important signaling molecule in the cardiovascular and nervous systems. H₂S donors reduce superoxide-induced endothelial damage²³ and have shown protective effects in animal models of inflammation and reperfusion injury^{23–26}. Therefore, H₂S donors may represent promising adjuvant therapies for DCS. Current treatment limitations highlight the need for new approaches, including H₂S donors such as GYY4137. This compound was selected for its bioavailability and rapid action²⁵ and has shown favorable results in preclinical myocardial ischemia-reperfusion models²⁶. It releases H₂S after two hydrolysis steps²⁷. H₂S may protect against ischemia/reperfusion, hypoxia, and ROS generation (see Fig. 1). Because cell death^{22, 28} and ROS production¹⁸ are implicated in DCS pathophysiology, further investigation of H₂S donors is warranted.

During cell death, adenosine deaminase (ADA) and xanthine oxidase (XO) drive purine degradation to uric acid. XO converts hypoxanthine to xanthine and xanthine to uric acid, producing reactive oxygen species (ROS) and altering cellular redox potential (see Fig. 1). Beyond its immune role, ADA, together with XO, regulates purine degradation flux, and both enzymes show increased activity during cell death²⁹ and see Fig. 1. This study aimed to evaluate (i) the effects of DCS on redox potential, ADA, and XO; (ii) the effects of H₂S donors on these parameters; and (iii) their protective effects against mortality in mice exposed to experimental DCS.

Results

Enzyme activities

ADA

After experimental DCS, mice treated with GYY4137 showed no significant difference in ADA activity compared to those injected with saline. However, the GY4137 group exhibited a higher median ADA than the controls (Fig. 2, left panel).

XO activity

After experimental DCS, XO activity was higher in mice injected with saline compared with controls. However, no significant difference was observed between mice injected with GYY4137 and those injected with saline (Fig. 2, right panel).

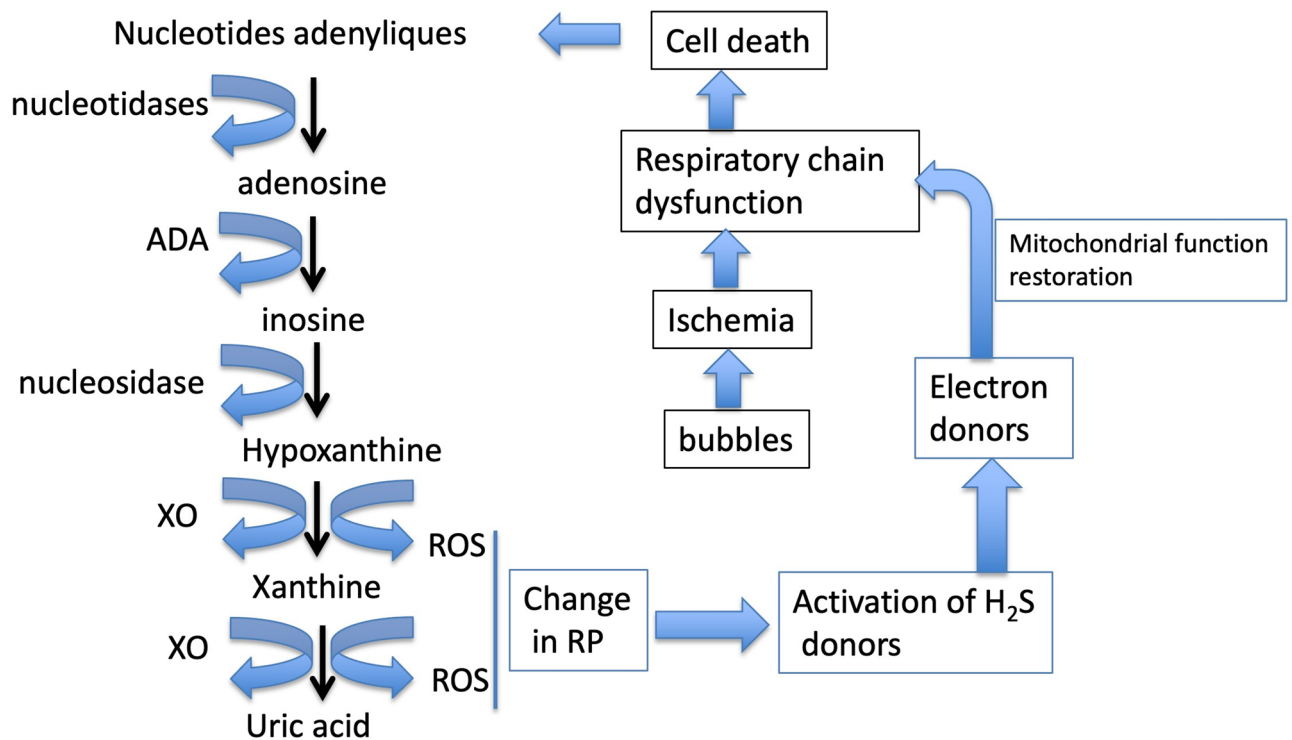


Fig. 1 Link between purine degradation pathway, ROS production and activation of H₂S donor during experimental DCS. H₂S release may protect against ischemia/hypoxia and ROS release. H₂S donor acts as electron donor to the respiratory chain of mitochondria to restore mitochondrial function RP: redox potential.

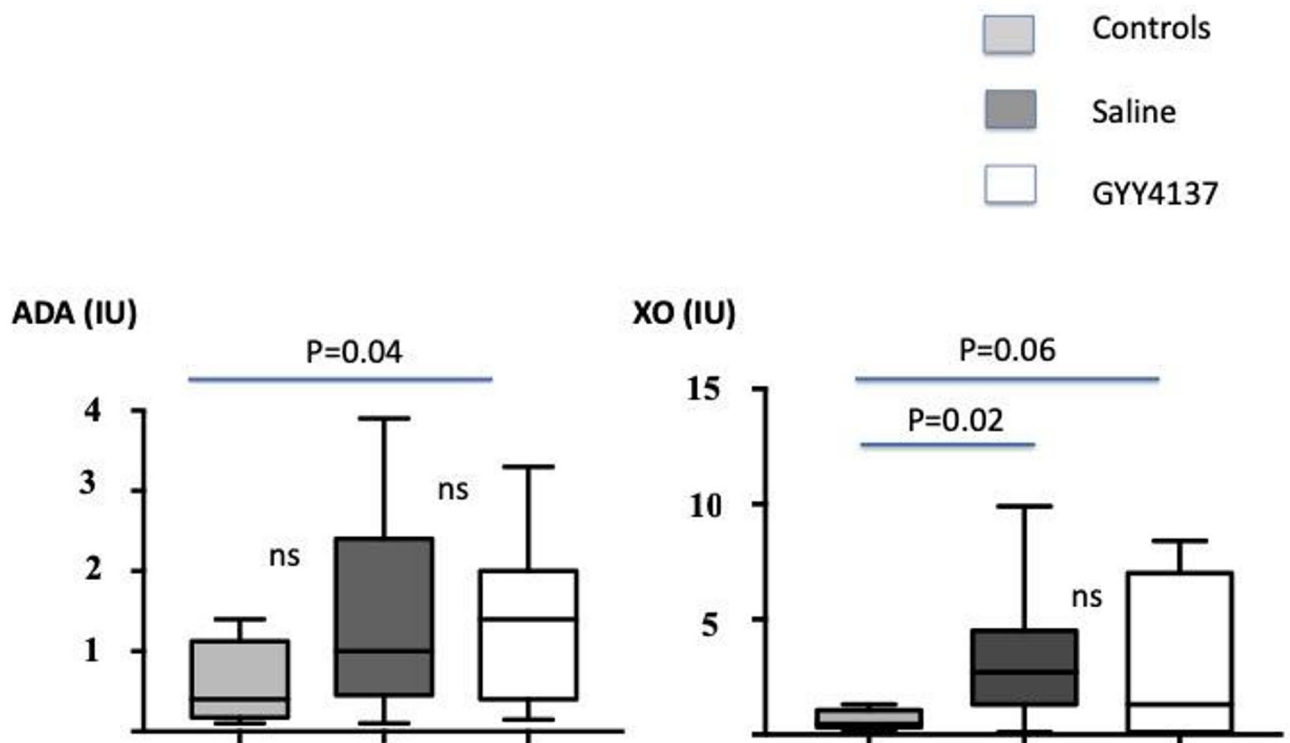


Fig. 2. Effects of experimental decompression sickness (DCS) on adenosine deaminase (ADA, left panel) and xanthine oxidase (XO, right panel) activities. Mice were injected intraperitoneally with GYY4137 (an H₂S donor, 50 mg/kg) or saline 30 min before decompression. Controls were mice injected with saline but not subjected to DCS. Comparisons between groups were performed using the Mann–Whitney test (n = 10 per group). IU: international units.

Redox potential

Following experimental DCS, mice injected with GYY4137 had a lower redox potential (RP, mV; mean – 29%) than those injected with saline (GYY4137: 116 [78–189] vs. saline: 150 [88–226], $p < 0.05$; see Fig. 3). However, the mean RP of the GYY4137 group remained higher than that of the saline group: 78.5 [68–110], $p < 0.01$.

Mortality of mice

The number of mice still alive in the different groups was 22 for GYY4137 and 14 for the saline group. The LD₅₀ measured with GY4137 was 13 ATA corresponding to 120 m depth (Table 1). Thus, LD₁₀₀ = LD₅₀ + a.b/n, where a is two ATA corresponding to 20-meter depth difference between the two pressures tested, b is the sum Σ of all the mice that survived, and n is the number of mice tested by depth (here 10).

The values were calculated using the Behrens and Karber Formula modified (see methods).

Discussion

The main result of this study is that the H₂S donor reduced the redox potential and improved survival in experimental DCS. These protective effects appear to be independent of purine pathway modulation, as the impact on the enzymes of this pathway is minimal.

H₂S is known as a gaseous signaling molecule that regulates numerous pathophysiological processes^{30,31} and affects respiratory and cardiovascular system homeostasis^{32,33}. It is an important independent mediator^{32,34,35}, also promoting NO-mediated effects on the cardiovascular system^{36,37}. H₂S has anti-inflammatory, antioxidative, and anti-apoptotic properties that protect against certain cardiovascular diseases, including ischemia-reperfusion^{37,38}. Blood pressure is reduced when H₂S acts on K⁺ channels, causing smooth muscle relaxation and vasodilation³⁹. H₂S donors inhibit superoxide-induced endothelial damage²³ and protect organs from ROS by activating nuclear factor erythroid 2-related factor 2 (Nrf2). Cell metabolism can also be affected by H₂S through modulation of mitochondrial respiration⁴⁰. An endogenous mechanism for H₂S production exists and involves the trans-sulfuration pathway, particularly cystathionine beta-synthase activity³⁰. In this case, the H₂S donor is homocysteine. This mechanism contributes to endogenous protective effects linked to H₂S release.

H₂S restores mitochondrial function and has cytoprotective effects through several mechanisms. The cardiovascular system appears to be a primary target, being positively influenced by H₂S both through vasodilation and blood pressure regulation, and at the cellular level by its antioxidative, anti-inflammatory, and cytoprotective properties⁴¹ (see Fig. 4). It has been shown that H₂S, while promoting apoptosis⁴², restores

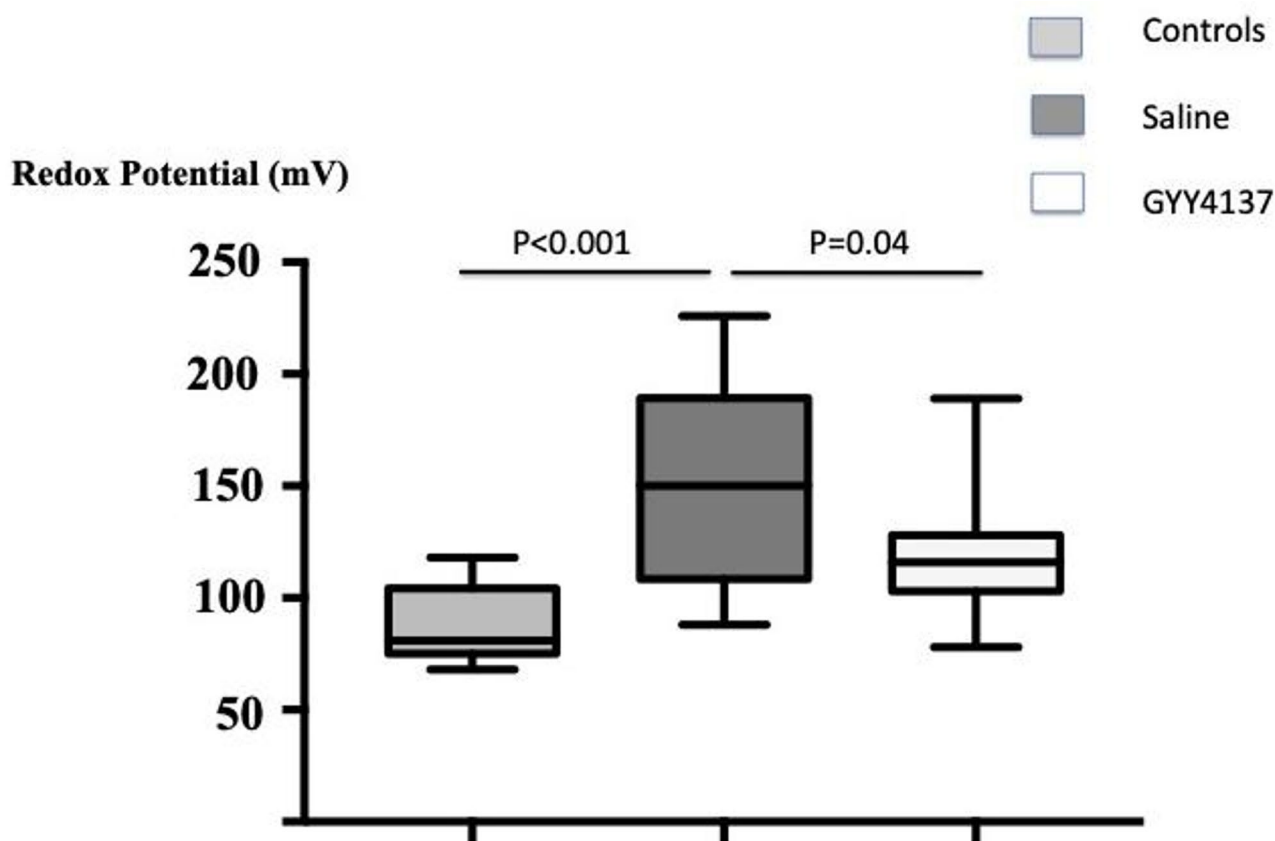


Fig. 3. Effects of experimental decompression sickness (DCS) on redox potential in mice ($n=10$ per group). Mice were injected intraperitoneally with either GYY4137 (50 mg/kg) or saline. Mann-Whitney test was performed for the comparison between groups.

ATA /depth	GY4137		Saline $p = 0.0038$	
	Dead mice (%)	Mice alive (number)	Dead Mice (%)	Mice alive (number)
9 /80	0	10	20	8
11/100	30	7	60	4
13/120	50	5	80	2

Table 1. Percentage of mice ($n = 10$ per group) dead after experimental decompression (1 min) as a function of environmental pressure expressed in ATA (atmosphere). Mice were injected intraperitoneally with saline (0.5 mL) or GYY4137 (50 mg/kg in 0.5 mL saline), a H_2S donor, half an hour before experimental decompression. During the decompression procedure the air flow was 500 to 600 l/min pending on suitable depth to reach atmospheric pressure (1 ATA) at the end. The Mann-Whitney test was used for the comparison between saline and CGS21680. The LD_{50} in the saline group was below 11 ATA (corresponding to a depth of 100 m), as 60% of mice died after the decompression procedure (Table 1). The calculated LD_{100} for the GYY4137 group (expressed as the equivalent depth) is $120 + 20 \times 22/10 = 144$ m. Assuming that the LD_{50} of the saline group is below 100 m (Table 1), the LD_{100} in this group would be below 128 m (Table 2).

	LD_{50}	LD_{100}
Saline	<100 m	<128 m
GY4137	120 m	144 m

Table 2. LD_{50} and LD_{100} of mice ($n = 30$ per group), submitted to experimental DCS.

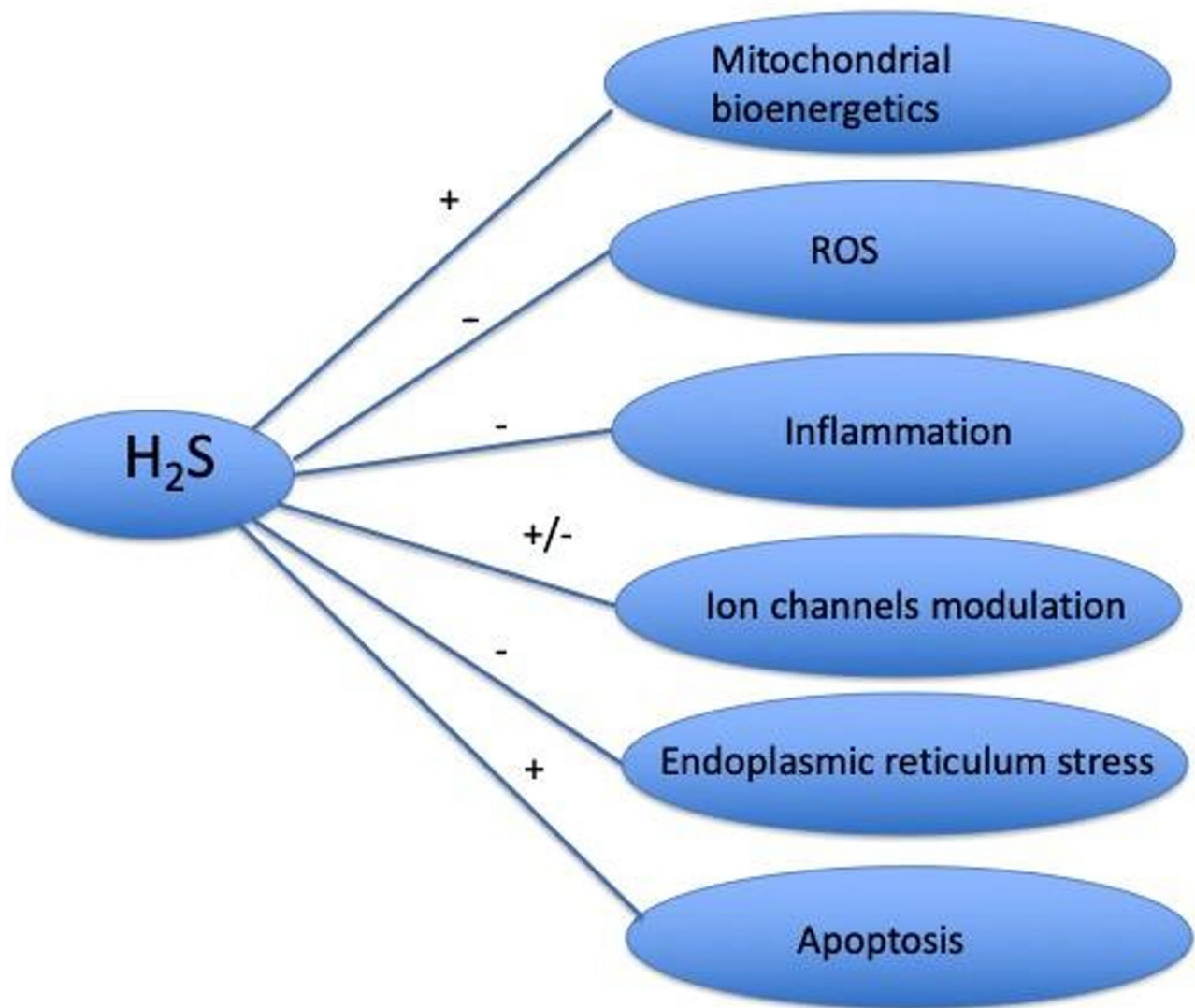


Fig. 4. Main targets of H₂S at a cellular level. H₂S while promoting apoptosis, restores mitochondrial function, inhibits ROS production, endoplasmic reticulum stress and inflammation partly through ion channels modulation.

mitochondrial energetics⁴³, inhibits ROS production in a model of myocardial ischemia-reperfusion^{26,44}, inhibits pro-inflammatory cytokine release⁴⁵, and reduces endoplasmic reticulum stress via phosphatase PTP1B⁴⁴. Part of these effects occurs through modulation of ion channels⁴⁶.

Besides bubbles, activation of the immune system and the formation of small particles (microparticles [MPs] or microvesicles) have been suggested to play an important role in decompression sickness (DCS) and in the generation of reactive oxygen species (ROS)⁴⁷.

Toxic ROS formation occurs through the activation of nitric oxide synthase and NADPH oxidase⁴⁸. NADPH oxidase, activated by neutrophils, generates ROS through myeloperoxidase activity⁴⁹. Therefore, granulocytes contribute to ROS production during the complex immune response that occurs in DCS⁴⁷.

Here, we found that GYY4137 lowered the redox potential in response to experimental DCS. However, redox potential is linked to ROS production, which occurs mainly through the first complex of the mitochondrial respiratory chain⁵⁰. We hypothesized that purine degradation is activated during DCS, resulting in ROS production. Indeed, purine degradation via the adenosine deaminase and xanthine oxidase pathways is a major source of ROS during cell death. DCS weakly modifies XO activity, suggesting that ROS production occurs independently of the purine degradation pathway and that, in our model, cell death is limited.

Finally, it has been shown that statins, through NO release, mitigate the risk and severity of DCS⁵¹, whereas agents that decrease NO production worsen DCS in female rats⁵². Antioxidant agents, such as vitamin C or N-acetylcysteine, while inhibiting ROS production in vitro, failed to produce conclusive results in vivo in rat models of DCS⁵³. The observed beneficial effects could be attributed to the multiple properties of GYY4137, namely its anti-radical, endothelial-protective, mitochondrial restoration function and vasodilatory activities,

as well as its ability to reduce redox potential. These properties could act synergistically, partly explaining the *in vivo* results.

Conclusion

We conclude that GYY4137 protects mice while also reducing redox potential and ROS production independently of the purine degradation pathway. Changes in enzymatic activities remain modest, however. In view of the numerous preclinical studies on sulfur donors, certain molecules could be tested not as preventive measures but as adjuvant treatments during decompression sickness (DCS).

Study limitations

We were unable to experimentally establish LD₁₀₀ because our system does not allow hyperbaric chamber decompression beyond 14 ATA in one minute. However, our investigation revealed a clear difference in the LD₅₀ value between mice injected with GYY4137 and those receiving the vehicle. Thus, LD₁₀₀ was calculated but not measured. Because nothing replaces experimentation, our results, particularly those concerning the calculation of LD₁₀₀ must be confirmed in an adequate hyperbaric chamber.

This study focuses on survival and redox potential but does not assess clinically relevant endpoints such as neurological deficits, motor function, or bubble formation. We cannot exclude the action of GYY4137 derivatives or metabolites in the observed effects. It should be noted that the protective effects of GYY4137 remain modest, and this work will need to be supplemented by mechanistic studies. Ultimately, our experimental model represents a rather severe decompression scenario that is only rarely encountered in humans, but this does not detract from the therapeutic properties of GYY4137 reported here. Finally, a precise study of the mechanisms underlying the protective effects of GYY4137 requires further investigation, which we now acknowledge as a limitation of this study.

Materials and methods

- Ethics and animals.

All animal-related procedures were in accordance with European (Directive 2010/63/EU) and French (Decree 2013/118) legislation. The Animal Ethics Committee (CE14, Aix-Marseille University) approved the protocol on May 6, 2022, under APAFIS#34720-2022011812031043. The study population consisted of 6-week-old male C57Bl/6n mice (males, 23 ± 2 g, from Charles River France). Animals were housed in an accredited animal facility with controlled temperature (22 ± 1 °C) and a day-night cycle (12 h of light per day, 7:00 am–7:00 pm). The mice had free access to water and to food (A03, UAR). They were acclimated for 6–7 days before the experiment.

- Drug exposition.

The mice were divided into three groups: a control group that had not been subjected to decompression sickness ($n = 10$) but who are injected intraperitoneally (i.p) with serum saline; two groups subjected to decompression sickness and previously injected i.p with saline solution ($n = 30$, 10 per hyperbaric condition, see hyperbaric procedure) or GYY4137 ($n = 30$).

Mice were injected intraperitoneally with GYY4137 (salt, Sigma Aldrich[®], Saint-Quentin-Fallavier, France) dissolved in 0.5 mL saline. We used only one dose (50 mg/kg) via the intraperitoneal route, which is a classic and optimal dosage for maximal prevention of ischaemia/reperfusion and ROS production^{54–56}. We used a dose of 50 mg/kg intraperitoneally (IP) in accordance with references^{54–56}. It appears that via this route, the protective effects are significant from 30 min up to at least 4 h (see⁵⁴). We injected GYY4137 thirty minutes before placing the animals in the chamber, with the animals remaining under high pressure for 1 h before decompression (see hyperbaric procedure), which means that the analysis of the results occurs 90 min after drug administration—therefore within an optimal window. Thirty minutes after the injection, the mice were subjected to the hyperbaric protocol. The mice were allowed to move freely in their cages. Ten mice not injected and not exposed to experimental DCS served as controls for biological parameters.

Hyperbaric procedure and LD₅₀

The procedure has been previously described^{11,57}. It seems intuitive that there is a relationship between depth, duration of exposure in hyperbaria, and decompression sickness. In fact, at constant exposure time and constant decompression speed (here, one minute), depth is the only variable that can be considered analogous to the toxic dose of a substance. This is why we considered using the Behrens and Karber formula, replacing the toxic dose with depth. Thus, the median lethal dose (LD₅₀) was calculated by increasing pressure in the hyperbaric chamber. We used the Behrens and Karber formula⁵⁸, originally adapted for drug toxicity⁵⁹, with some modifications⁶⁰. The LD₁₀₀ was defined as the minimum depth leading to 100% mortality after one minute of decompression, and the mice were observed for 30 min after the decompression procedure.

We replaced the toxin dose with the environmental pressure (ATA) corresponding to depth:

$$LD_{50} = LD_{100} - a \cdot b/n.$$

where a is the difference in depth between two trials (2 ATA, corresponding to a difference of 20 m depth), b is the sum (Σ) of all mice remaining alive between the two depths, and n is the number of mice tested at each depth (here, 10).

Thirty minutes after injection, two cages of mice, each containing five animals, were placed in a 50-liter hyperbaric chamber for 1 h at maximal pressure. Air compression (diving air, Air Liquide France) included two ramps of pressure increase: first, at 0.1 ATA/min up to a pressure of 2 ATA (absolute atmosphere), followed

by 1 ATA/min up to the maximum tested. During the decompression procedure, airflow was 500–600 l/min, depending on the depth, to reach atmospheric pressure (1 ATA) at the end. In summary, three pressure conditions (9, 11, and 13 ATA) were tested, with atmospheric pressure serving as the control group. Decompression was performed over 1 min to induce severe experimental DCS, as previously described^{11,57}. Mice were observed for 30 min after experimental DCS. All experiments were repeated twice, with 10 mice per treatment.

Anesthesia and blood sample collection

Animals were initially anesthetized in an individual cage with gaseous isoflurane (4.0% in oxygen flow at 2.0 l/min) for 2 min, then maintained through a face mask (Anesthetizing Box; Harvard Apparatus, Les Ulis, France). An intraperitoneal injection of ketamine (100 mg·kg⁻¹) and xylazine (10 mg·kg⁻¹) completed anesthesia. The anesthesia level was confirmed by testing the absence of withdrawal reflexes in response to pinching the distal hind limbs.

Immediately after anesthesia, blood samples were collected via intracardiac puncture for ADA, XO, and redox assays. Blood was collected in a sterile 1 ml syringe containing lithium heparin, immediately placed on ice, and processed according to the manufacturer's instructions. Finally, animal euthanasia was performed after intraperitoneal injection of ketamine and xylazine at a lethal dose.

- ADA measurement.

ADA levels were measured as described⁶¹. Adenosine deaminase catalyzes the deamination of adenosine to inosine by forming ammonium (NH₄⁺) in a stoichiometric ratio. Briefly, adenosine (750 μL, 28 mM) was incubated with plasma (125 μL) in saline (125 μL, 7% BSA) for 37 min at 37 °C. The reaction was initiated by adding adenosine and terminated in ice water. The ammonia produced by ADA was measured using an Atelica analyzer (Siemens, Erlangen, Germany) and expressed in international units per liter (IU).

- Xanthine oxidase measurement.

XO content was evaluated as previously described⁶². Briefly, 200 μL of xanthine (0.5 mmol/L dissolved in *saline*, Sigma-Aldrich) and 100 μL of adenosine triphosphate (300 μmol/L dissolved in *saline*) were mixed with 0.3 mL of serum. After incubation (37 °C for 30 min), the uric acid present was measured using a DX Beckman Coulter apparatus (Danaher Corporation, Washington DC, USA).

- Redox potential measurement.

To measure the redox potential, we used the SEN 0464 probe (indicator electrode platinum; reference electrode silver-silver chloride; DFROBOT, Gotronic, France). An automatic three-point calibration was performed, with the range set at -2000 to +2000 mV. The intra-assay coefficient of variation was <10 mV, and the internal resistance was <10 kOhms as per the manufacturer's recommendations. 50 μL of plasma per mouse was tested. The samples were analyzed in the same time in a controlled temperature box (23 °C), temperature being controlled using a temperature probe.

Statistical Analyses

Data are expressed as the median and range. A Mann Whitney test was used to compare biological variables between groups of mice. Statistical significance was set at $p < 0.05$.

Number of mice: We determined that, with a 5% alpha risk and a 25% difference in mean mortality, the required number of mice is 10 per group. Regarding enzyme activities, considering that a 50% difference is of interest, 8 mice per group are required.

Data availability

The datasets generated and/or analysed during the current study available from the corresponding author.

Received: 3 July 2025; Accepted: 19 February 2026

Published online: 05 March 2026

References

1. Mitchell, S. J., Bennett, M. H. & Moon, R. E. Decompression Sickness and Arterial Gas Embolism. *N Engl. J. Med.* **386**, 1254–1264 (2022).
2. Vann, R. D., Butler, F. K., Mitchell, S. J. & Moon, R. E. Decompression illness. *Lancet* (2011). 377,153–64.
3. Simonnet, B. et al. Therapeutic management of severe spinal cord decompression sickness in a hyperbaric center. *Front Med* **10**, 1172646 (2023). (2023).
4. Bessereau, J. et al. Place de l'aspirine dans le traitement médicamenteux de l'accident de désaturation. *Thérapie* **63**, 419–423 (2008).
5. Lambrechts, K. et al. Tirofiban, a Glycoprotein IIb/IIIa Antagonist, Has a Protective Effect on Decompression Sickness in Rats: Is the Crosstalk Between Platelet and Leukocytes Essential? *Front. Physiol.* **9**, 906 (2018).
6. Lambrechts, K. et al. Mechanism of action of antiplatelet drugs on decompression sickness in rats: a protective effect of anti-GPIIb/IIIa therapy. *J. Appl. Physiol.* **118**, 1234–1239 (2015).
7. Pontier, J. M., Vallee, N., Ignatescu, M. & Bourdon, L. Pharmacological intervention against bubble-induced platelet aggregation in a rat model of decompression sickness. *J. Appl. Physiol.* **110**, 724–729 (2011).
8. Duplessis, C. A., Fothergill, D., Schwaller, D., Hughes, L. & Gertner, J. Prophylactic statins as a possible method to decrease bubble formation in diving. *Aviat. Space Environ. Med.* **78**, 430–434 (2007).
9. Zhang, K. et al. Simvastatin decreases incidence of decompression sickness in rats. *Undersea Hyperb Med.* **42**, 115–123 (2015).
10. Blatteau, J. E., Brubakk, A. O., Gempp, E., Castagna, O. & Risso, J. J., Vallée, N. Sildenafil pre-treatment promotes decompression sickness in rats. *PLoS One.* **8**, e60639 (2013).

11. Vallee, N. et al. Fluoxetine Protection in Decompression Sickness in Mice is Enhanced by Blocking TREK-1 Potassium Channel with the spadin Antidepressant. *Front. Physiol.* **7**, 42 (2016).
12. Blatteau, J. E. et al. *K Xenon Blocks Neuronal Injury Associated with Decompression. Sci Rep* **5**, 15093 (2015).
13. Sheppard, R. L., Regis, D. P. & Mahon, R. T. Dodecafluoropentane (DDFPe) and decompression sickness-related mortality in rats. *Aviat. Space Environ. Med.* **86**, 21–26 (2015).
14. Forbes, A. S., Regis, D., Hall, A. A., Mahon, R. T. & Cronin, W. Propranolol Effects on Decompression Sickness in a Simulated DISSUB Rescue in Swine. *Aero Med. Hum. Perf.* **88**, 385–391 (2017).
15. Kizer, K. W. Corticosteroids in treatment of serious decompression sickness. *Annals Emerg. Med.* **10**, 485–488 (1981).
16. Bennett, M., Mitchell, S. & Dominguez, A. Adjunctive treatment of decompression illness with a non-steroidal anti-inflammatory drug (tenoxicam) reduces compression requirement. *Undersea Hyperb. Med.* **30**, 195–206 (2003).
17. Zhang, K. et al. Endothelial dysfunction correlates with decompression bubbles in rats. *Sci. Rep.* **6**, 33390 (2016).
18. Wang, Q. et al. Reactive Oxygen Species, Mitochondria, and Endothelial Cell Death during In Vitro Simulated Dives. *Med. Sci. Sports Exerc.* **47**, 1362–1371 (2015).
19. Mrkac-Sposta, S. et al. Change in oxidative stress biomarkers during 30 days in saturation dive: A pilot study. *Int. J. Env Res. Public Health.* **17**, 7118 (2020).
20. Magri, K. et al. Pace, N.P. Acute effects on the human peripheral blood transcriptome of decompression sickness secondary to scuba diving. *Front. Physiol.* **12**, 660402 (2021).
21. Wang, B. et al. ROS-induced lipid peroxidation modulates cell death outcome: mechanisms behind apoptosis, autophagy, and ferroptosis. *Arch. Toxicol.* **97**, 1439–1451 (2023).
22. Vallée, N., Gaillard, S., Peinnequin, A., Rissoff, J. & Blatteau, J.E. Evidence of cell damages caused by circulating bubbles: high level of free mitochondrial DNA in plasma of rats. *J. Appl. Physiol.* (1985). **115**, 1526–1532 (2013).
23. Marini, E. et al. Comparative Study of Different H₂S Donors as Vasodilators and Attenuators of Superoxide-Induced Endothelial Damage. *Antioxidants* **12**, 344 (2023).
24. Szabó, C. Hydrogen sulphide and its therapeutic potential. *Nat. Rev. Drug Discovery.* **6**, 917–935 (2007).
25. Harper, A. et al. GYY4137, a hydrogen sulfide donor, protects against endothelial dysfunction in porcine coronary arteries exposed to myeloperoxidase and hypochlorous acid. *Vascul Pharmacol.* **152**, 107199. <https://doi.org/10.1016/j.vph.2023.107199> (2023).
26. Qiu, Y. Y. et al. GYY4137 protects against myocardial ischemia/reperfusion injury via activation of the PHLPP-1/Akt/Nrf2 signaling pathway in diabetic mice. *J. Surg. Res.* **225**, 29–39 (2018).
27. Alexander, B. E. et al. Investigating the generation of hydrogen sulfide from the phosphoramidodithioate slow release donor GYY4137. *Med. Chem. Com.* **6**, 1649–1655 (2015).
28. Wang, Q. et al. Reactive Oxygen Species, Mitochondria, and Endothelial Cell Death during In Vitro Simulated Dives. *Med. Sci. Sports Exerc.* **47**, 1362–1371 (2015).
29. Newsholmes and Leech: In. *Biochemistry for the medical sciences* (Wiley, 1983).
30. Corvino, A. et al. Severino, B. Trends in H₂S-donors chemistry and their effects in cardiovascular diseases. *Antioxidants* **10**, 429 (2021).
31. Moore, P. K., Bhatia, M. & Mochhala, S. Hydrogen sulfide: from the smell of the past to the mediator of the future? *Trends Pharmacol. Sci.* **24**, 609–611 (2003).
32. Li, L., Rose, P. & Moore, P. K. Hydrogen sulfide and cell signaling. *Annu. Rev. Pharmacol. Toxicol.* **51**, 169–187 (2011).
33. Wang, Q., Wang, X. L., Liu, H. R., Rose, P. & Zhu, Y. Z. Protective effects of cysteine analogues on acute myocardial ischemia: novel modulators of endogenous H₂S production. *Antioxid. Redox Signal.* **12**, 1155–1165 (2010).
34. Kolluru, G. K., Shackelford, R. E., Shen, X., Dominic, P. & Kevil, C. G. Sulfide regulation of cardiovascular function in health and disease. *Nat. Reviews Cardiol.* **20**, 109–125 (2023).
35. Liu, Y. H. et al. Hydrogen sulfide in the mammalian cardiovascular system. *Antioxid. Redox. Signal.* **17**, 141–185 (2012).
36. Pan, L. L., Qin, M., Liu, X. H. & Zhu, Y. Z. The role of hydrogen sulfide on cardiovascular homeostasis: an overview with update on immunomodulation. *Front. Pharmacol.* **8**, 686 (2017).
37. Calvert, J. W., Coetzee, W. A. & Lefer, D. J. Novel insights into hydrogen sulfide-mediated cytoprotection. *Antioxid. Redox. Signal.* **12**, 1203–1217 (2010).
38. Yu, X. H. et al. Hydrogen sulfide as a potent cardiovascular protective agent. *Clin. Chim. Acta.* **437**, 78–87 (2014).
39. Yuan, S., Shen, X. & Kevil, C. G. Beyond a gasotransmitter: hydrogen sulfide and polysulfide in cardiovascular health and immune response. *Antioxid. Redox. Signal.* **27**, 634–653 (2017).
40. Sanchez-Aranguren, L. C. et al. Bioenergetic effects of hydrogen sulfide suppress soluble Flt-1 and soluble endoglin in cystathionine gamma-lyase compromised endothelial cells. *Sci. Rep.* **10**, 15810. <https://doi.org/10.1038/s41598-020-72371-2> (2020).
41. Hu, Q. & Lukesh, J. C. 3 rd. H₂S Donors with Cytoprotective Effects in Models of MI/R Injury and Chemotherapy-Induced Cardiotoxicity. *Antioxidants (Basel)*. **12**, 650. (). (2023).
42. Yang, G., Wu, L. & Wang, R. Pro-apoptotic effect of endogenous H₂S on human aorta smooth muscle cells. *FASEB J.* **20**, 553–555 (2006).
43. Módis, K., Wolanska, K. & Vozdek, R. Hydrogen sulfide in cell signaling, signal transduction, cellular bioenergetics and physiology in *C. elegans*. *Gen Physiol Biophys.* **32**, 1–22 (2013).
44. Kabil, O., Motl, N. & Banerjee, R. H₂S and its role in redox signaling. *Biochim. Biophys. Acta.* **1844**, 1355–1366 (2014).
45. Whiteman, M. et al. The effect of hydrogen sulfide donors on lipopolysaccharide-induced formation of inflammatory mediators in macrophages. *Antioxid. Redox Signal.* **12**, 1147–1154 (2010).
46. Peers, C., Bauer, C. C., Boyle, J. P., Scragg, J. L. & Dallas, M. L. Modulation of ion channels by hydrogen sulfide. *Antioxid. Redox Signal.* **17**, 95–105 (2012).
47. Schirato, S. R. et al. A broad appraisal of decompression-induced physiological stress in different simulated dive profiles. *J. Clin. Trans. Res.* **10**, 269–282 (2024).
48. Thom, S. R., Bhopale, V. M. & Yang, M. Neutrophils generate microparticles during exposure to inert gases due to cytoskeletal oxidative stress. *J. Biol. Chem.* **288**, 18831–18845 (2014).
49. Winterbourn, C. C., Kettle, A. J. & Hampton, M. B. Reactive Oxygen Species and Neutrophil Function. *Annu. Rev. Biochem.* **85**, 765–792 (2016).
50. Okoye, C. N., Koren, S. A. & Wojtovich, A. P. Mitochondrial complex I ROS production and redox signaling in hypoxia. *Redox Biol.* **67**, 102926 (2023).
51. Duplessis, C. A. & Fothergill, D. Investigating the potential of statin medications as a nitric oxide (NO) release agent to decrease decompression sickness: a review article. *Med. Hypotheses.* **70**, 560–566 (2008).
52. Mazur, A. et al. Different effect of l-NAME treatment on susceptibility to decompression sickness in male and female rats. *Appl. Physiol. Nutr. Metab.* **39**, 1280–1285 (2014).
53. Wang, Q. et al. Antioxidants, endothelial dysfunction, and DCS: in vitro and in vivo study. *J. Appl. Physiol.* **119**, 1355–1362 (1985).
54. Veskemaa, L., Taher, M., Graw, J. A., Gonzalez-Lopez, A. & Francis, R. C. E. Slow releasing sulphide donor GYY4137 protects mice against ventilator-induced lung injury. *Intensive Care Med. Exp.* **13**, 45 (2025).
55. Qiu, Y. et al. GYY4137 protects against myocardial ischemia/reperfusion injury via activation of the PHLPP-1/Akt/Nrf2 signaling pathway in diabetic mice. *J. Surg. Res.* **225**, 29–39 (2018).
56. Liu, Z. et al. The hydrogen sulfide donor, GYY4137, exhibits anti-atherosclerotic activity in high fat fed apolipoprotein E(-/-) mice. *Br. J. Pharmacol.* **169**, 1795–1809 (2013).

57. Blatteau, J. E. et al. Vallee, N. Protective effects of fluoxetine on decompression sickness in mice. *PLoS One*. **7**, e49069 (2012).
58. Behrens, B. & Karber, C. How arrange most convenient series of biological tests for evaluations. *Archiv für Exp. Pathol. und Pharmak.* **177**, 379–388 (1935).
59. Guieu, R., Kopeyan, C. & Rochat, H. Utilization of aspirin, quinine and verapamil in the prevention and treatment of scorpion venom intoxication. *Life Sci.* **53**, 1935–1946 (1993).
60. Randhawa, M. A. Calculation of LD50 values from the method of Miller and Tainter, 1944. *J. Ayub Med. Coll. Abbottabad.* **21**, 184–185 (2009).
61. Sampol, J. et al. High adenosine and deoxyadenosine concentrations in mononuclear cells of hemodialyzed patients. *J. Am. Soc. Nephrol.* **12**, 1721–1728 (2001).
62. Gondouin, B. et al. Plasma xanthine oxidase activity is predictive of cardiovascular disease in patients with chronic kidney disease, independently of uric acid levels. *Nephron* **131**, 167–174 (2015).

Author contributions

L.D.; N.V.; J.E.B.; J.J.R.; J.C.R.; R.G: Conception, design and writing the paper M.M.; H.L.; A.B: performed the experiments S.C.; M.G.; J.S.D.; S.L. J.F: Data collection and interpretation All authors have read and approved the manuscript.

Declarations

Competing Interests

The authors declare that the research was conducted in the absence of any commercial or financial relationships that could be construed as a potential conflict of interest.

Ethics statement

The protocol obtained approval from the animal ethics committee (CE14, Aix-Marseille University) on May 6, 2022 under number APAFIS#34720-2022011812031043. Institutional Review Board Statement: All procedures involving animals comply with European (Directive 2010/63/EU) and French (Decree 2013/118) legislation. The protocol was approved by the Animal Etic Comitee (CE 14 of AMU) on may 6, 2022. This study is in accordance with ARRIVE guidelines

Additional information

Correspondence and requests for materials should be addressed to R.G.

Reprints and permissions information is available at www.nature.com/reprints.

Publisher's note Springer Nature remains neutral with regard to jurisdictional claims in published maps and institutional affiliations.

Open Access This article is licensed under a Creative Commons Attribution-NonCommercial-NoDerivatives 4.0 International License, which permits any non-commercial use, sharing, distribution and reproduction in any medium or format, as long as you give appropriate credit to the original author(s) and the source, provide a link to the Creative Commons licence, and indicate if you modified the licensed material. You do not have permission under this licence to share adapted material derived from this article or parts of it. The images or other third party material in this article are included in the article's Creative Commons licence, unless indicated otherwise in a credit line to the material. If material is not included in the article's Creative Commons licence and your intended use is not permitted by statutory regulation or exceeds the permitted use, you will need to obtain permission directly from the copyright holder. To view a copy of this licence, visit <http://creativecommons.org/licenses/by-nc-nd/4.0/>.

© The Author(s) 2026